

Comparison of viscous and kinetic dynamic relaxation methods in form-finding of membrane structures

S. Fatemeh Labbafi^{1a}, S. Reza Sarafrazi^{1b} and Thomas H.-K. Kang^{*2,3}

¹Department of Civil Engineering, University of Birjand, Birjand, Iran

²Department of Architecture & Architectural Engineering, Seoul National University, Seoul, Korea

³Department of Civil and Environmental Engineering, University of Illinois at Urbana-Champaign, USA

(Received October 31, 2016, Revised December 19, 2016, Accepted December 22, 2016)

Abstract. This study focuses on the efficiency and applicability of dynamic relaxation methods in form-finding of membrane structures. Membrane structures have large deformations that require complex nonlinear analysis. The first step of analysis of these structures is the form-finding process including a geometrically nonlinear analysis. Several numerical methods for form-finding have been introduced such as the dynamic relaxation, force density method, particle spring systems and the updated reference strategy. In the present study, dynamic relaxation method (DRM) is investigated. The dynamic relaxation method is an iterative process that is used for the static equilibrium analysis of geometrically nonlinear problems. Five different examples are used in this paper. To achieve the grading of the different dynamic relaxation methods in form-finding of membrane structures, a performance index is introduced. The results indicate that viscous damping methods show better performance than kinetic damping in finding the shapes of membrane structures.

Keywords: dynamic relaxation method; viscous damping; kinetic damping; form-finding; membrane structures

1. Introduction

The dynamic relaxation method (DRM) is an iterative process that is used in solving the system of equations. For static equilibrium equations, by adding the fictitious mass and damping terms, the DRM converts the static to dynamic state (Rezaiee-Pajand and Sarafrazi 2011). Rooted in the 2nd-order Richardson method is the mathematical basis of DRM (Frankel 1950). The DRM was proposed for the first time by Otter, who emphasized the DRM capability based on a comparison between DRM and any other iterative method (Otter 1966). Many researchers have used this method for analyzing linear systems. Twelve existing and new dynamic relaxation methods based on the number of iterations and overall analysis duration were introduced by Rezaiee-Pajand *et al.* (2012). Rushton (Rushton 1969), Brew and Brotton (Brew and Brotton 1971), Wood (Wood 1971)

*Corresponding author, Associate Professor, E-mail: tkang@snu.ac.kr

^aM.Sc., E-mail: sf.labbafi@yahoo.com

^bAssistant Professor, E-mail: srsarafrazi@birjand.ac.ir

and Bunce (Bunce 1972) used this method for solving linear and nonlinear systems. Additionally, the kinetic damping theory was proposed by Cundall, who, by eliminating of damping, changed the procedure of DRM (Cundall 1976). In 2008, the method was modified by Topping and Ivanyi (2008). Then Cassell and Hobbs (Cassell and Hobbs 1976), Frieze *et al.* (Frieze *et al.* 1978), Papadrakakis (Papadrakakis 1981), Qiang (Qiang 1988), Al-Shawi and Mardirosian (Al-Shawi and Mardirosian 1987) and many other researchers have improved fictitious mass, damping and time for DRM (Munjiza *et al.* 1998; Rezaiee Pajand and Alamatian 2010, Rezaiee-Pajand and Sarafrazi 2010, Zhang and Yu 1989). For improving the accuracy further, Rezaiee-Pajand and Taghavian-Hakkak (2006) employed the three terms of Taylor series and formulated a new DRM process. For the optimal time step, Kadkhodayan *et al.* (2008) minimized the residual force. Also, the optimum time step by means of utilizing minimum energy was presented by Rezaiee Pajand and Alamatian (2005). In 2010s, Rezaiee-Pajand and Sarafrazi (2010) investigated the DRM algorithms and proposed a general formulation, and by setting the damping factor to zero they also proposed an alternative DRM algorithm that did not require the damping factor (Rezaiee-Pajand and Sarafrazi 2011). Furthermore, Rezaiee-Pajand *et al.* (2011) proposed a newer technique for updating the damping factor, where the convergence rate was improved. Recently, Alamatian (2012) presented a new relationship for fictitious mass of kinetic damping based on running an incremental analysis, and Rezaiee-Pajand and Rezaee (2014) introduced a new formula based upon error analysis for the time step of the algorithm.

The form-finding is a process of finding the basic static shape of the structure taking into account pre-tension forces only. It is done before a detailed analysis, involving imposed loads such as snow and wind (Lewis 2003, Xu *et al.* 2015). Barnes (1998) discussed about the use of kinetic DRM in form-finding of prestressed nets and membranes, while Wood (2002) introduced a simple technique for form-finding of membranes using DRM. Also, Veenendaal and Block (2012) compared various form-finding methods such as DRM and others for discrete networks. Nabaei *et al.* (2013) proposed a modified dynamic relaxation method with a fictitious stiffness-proportional damping into an equivalent fictitious viscous material model for form-finding of timber fabric structures.

In this paper, two plans relating to membrane structures are loaded and form-finding of them is determined by dynamic relaxation method. Five methods of dynamic relaxation including traditional Dynamic Relaxation method (DR), Modified Dynamic Relaxation methods (MDR1 and MDR2), Kinetic Dynamic Relaxation method (KDR), and Kinetic Dynamic Relaxation with Time step method (KDRT) are used, and the number of iterations and CPU time of these methods are recorded. These methods are used for finding shapes of five membrane examples.

2. Dynamic relaxation methods

2.1 Traditional Dynamic Relaxation method (DR)

In the traditional dynamic relaxation method (DR), a static system is transferred to the artificial dynamic space by adding artificial inertia and damping forces as follows (Rezaiee Pajand and Taghavian Hakkak 2006)

$$\mathbf{M}\ddot{\mathbf{X}} + \mathbf{C}\dot{\mathbf{X}} + \mathbf{S}\mathbf{X} = \mathbf{P} \quad (1)$$

In this equation, \mathbf{M} , \mathbf{C} and \mathbf{K} are the mass, damping, and stiffness matrices, respectively; \mathbf{X}

is the displacement vector; and $\ddot{\mathbf{X}}$ and $\dot{\mathbf{X}}$ are the acceleration and velocity vectors, respectively. For the formulation of a dynamic relaxation, numerical techniques are used. Using the finite difference method and according to the form, the velocity and acceleration vectors can be written as follows

$$\dot{\mathbf{X}}^{n+1/2} = \frac{1}{\tau^{n+1}} (\mathbf{X}^{n+1} - \mathbf{X}^n) \quad (2)$$

$$\dot{\mathbf{X}}^n = \frac{1}{2} (\dot{\mathbf{X}}^{n-1/2} + \dot{\mathbf{X}}^{n+1/2}) \quad (3)$$

$$\ddot{\mathbf{X}}^n = \frac{1}{\tau^n} (\dot{\mathbf{X}}^{n+1/2} - \dot{\mathbf{X}}^{n-1/2}) \quad (4)$$

where τ is the time step and n is the iteration of DRM.

Typically, the damping matrix is defined as a multiple of the mass matrix. This equation of damping can be written as $\mathbf{C} = c\mathbf{M}$, where c is the damping factor. With replacement values of velocity and acceleration and damping matrix in dynamic systems, the velocity in time $t^{n+1/2}$ is obtained

$$\begin{aligned} \{\dot{\mathbf{X}}\}^{n+1/2} &= \frac{2 - \tau^n c^n}{2 + \tau^n c^n} \{\dot{\mathbf{X}}\}^{n-1/2} + \frac{2\tau^n}{2 + \tau^n c^n} [\mathbf{M}]^{-1} \{\mathbf{R}\} \\ &= \frac{2 - \tau^n c^n}{2 + \tau^n c^n} \{\dot{\mathbf{X}}\}^{n-1/2} + \frac{2\tau^n}{2 + \tau^n c^n} \left\{ \begin{matrix} R_i \\ m_{ii} \end{matrix} \right\}^n \end{aligned} \quad (5)$$

$$\{\mathbf{X}\}^{n+1} = \{\mathbf{X}\}^n + \tau^{n+1} \{\dot{\mathbf{X}}\}^{n+1/2} \quad (6)$$

In these equations, m_{ii}^n and r_{ii}^n are the i -th diagonal element of mass matrix and residual force for i -th degree of freedom, respectively. The residual force in n -th step is calculated by the following equation

$$\{\mathbf{R}\}^n = \{\mathbf{P}\}^n - \{\mathbf{f}\}^n = [\mathbf{M}]\{\ddot{\mathbf{X}}\}^n + [\mathbf{C}]\{\dot{\mathbf{X}}\}^n \quad (7)$$

where \mathbf{R} , \mathbf{P} and \mathbf{f} are the residual, external and internal forces, respectively.

In this equation, mass matrix, damping factor and time step are unknown. One of the most common approaches to determine the fictitious mass matrix is using the Gerschgorin's theory (Cassell and Hobbs 1976). This scheme gives the following expression for the i -th diagonal element of the mass matrix

$$m_{ii} = \frac{(\tau^n)^2}{4} \text{Max} \left[\sum_{i=1}^{ndof} |S_{ij}|, 2S_{ii} \right] \quad (8)$$

In this article, the second formulation for fictitious mass matrix in all methods is used. In this equation, $ndof$ is the number of degrees of freedoms and \mathbf{S} is the stiffness matrix.

According to the theory of structural dynamics, if damping is critical, the convergence rate is maximum response. Thus to estimate the critical damping, Rayleigh's principle is used

$$c^n = 2 \sqrt{\frac{\left(\{\mathbf{X}\}^n \right)^T \{ \mathbf{f}(\{\mathbf{X}\}^n) \}}{\left(\{\mathbf{X}\}^n \right)^T [\mathbf{M}] \{\mathbf{X}\}^n}} \quad (9)$$

In addition, other methods to determine the damping factor are available. In many DRMs, time step is assumed to be constant and equal to one. However, other methods for determining the time step on the Rayleigh's principle are also suggested (Papadrakakis 1981), as well as the improved time step formulated by minimizing the residual force (Kadkhodayan *et al.* 2008). The general DRM algorithm is given (Rezaiee-Pajand *et al.* 2012), as follows

1. Defining ε_r , \mathbf{X}^0 , $\dot{\mathbf{X}}^{-1/2} = 0$ and τ^0
2. $n = 1$
3. Assembling the internal force vector and applying boundary conditions
4. Evaluating the residual forces, artificial mass matrix and damping factor
5. Updating the value of time step τ
6. Calculating $\dot{\mathbf{X}}^{n+1/2}$ and \mathbf{X}^{n+1}
7. If $\|\mathbf{R}^{n+1}\| \leq \varepsilon_r$, then stopping the algorithm
8. $n = n + 1$
9. If $n \leq N_{\max}$, continuing the DRM iteration from step 3.

Here, N_{\max} is the maximum allowable number of iterations, which should be defined by the analyst, and ε_r is the maximum allowable error of displacement.

2.2 Modified Dynamic Relaxation method (MDR)

In 2002, Rezaiee-Pajand and Alamatian performed an error analysis on the DRM and suggested another mass matrix as below (Rezaiee Pajand and Alamatian 2010) (MDR1)

$$m_{ii} = \max \left\{ \frac{(\tau^n)^2}{2} s_{ii}, \frac{(\tau^n)^2}{4} \sum_{i=1}^{ndof} |S_{ij}| \right\} \quad i = 1, 2, \dots, ndof \quad (10)$$

They also employed new formulation to calculate damping factor. Furthermore, the lowest circular frequency is calculated via the following equation (Rezaiee Pajand and Alamatian 2010) (MDR2)

$$c = \sqrt{\omega_0^2 \left[4 - (h^k)^2 \omega_0^2 \right]} \quad (11)$$

$$\omega_0 = \sqrt{\frac{\left(\{\mathbf{X}\}^n \right)^T \{ \mathbf{f}(\{\mathbf{X}\}^n) \}}{\left(\{\mathbf{X}\}^n \right)^T [\mathbf{M}] \{\mathbf{X}\}^n}} \quad (12)$$

2.3 Kinetic Dynamic Relaxation method (KDR)

The method of kinetic damping does not require fictitious damping matrix. Hence, only the time step and the fictitious nodal masses are required. In this way the time step interval may be fixed and the masses estimated from Eq. (8) or Eq. (10). With kinetic energy damping the velocities of the joints are set to zero when a fall in the level of total kinetic energy of the structure occurs. This fall in the kinetic energy indicates that a peak has been passed. If this peak is detected by a fall in kinetic energy at time $n + 1/2$ then since the current coordinates are calculated at the same time as the velocities, the current coordinates stored in the vectors will be $\mathbf{X}^{n+1/2}$. If these coordinates are adopted as the starting position for the next cycle of calculation then full convergence may not necessarily be achieved. The coordinates are set to $\mathbf{X}^{n-1/2}$ when the peak is assumed to have occurred (Topping and Ivanyi 2008). Fig. 1 shows variation of kinetic energy in kinetic dynamic relaxation methods.

$$\mathbf{X}^{n-1/2} = \mathbf{X}^{n+1} - \frac{3\tau \dot{\mathbf{X}}^{n+1/2}}{2} + \frac{\tau^2 \mathbf{R}^n}{2\mathbf{M}} \quad (13)$$

When the analysis is restarted, the velocities must be calculated at the mid-point of the first time step as follows

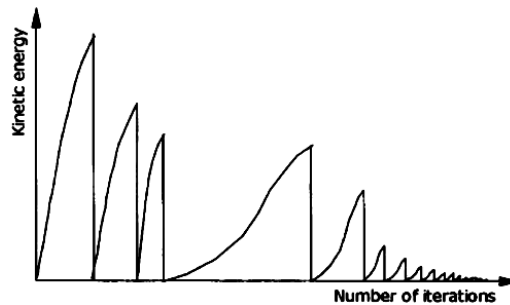


Fig. 1 Variation in kinetic energy in dynamic relaxation algorithm (Cundall 1976)

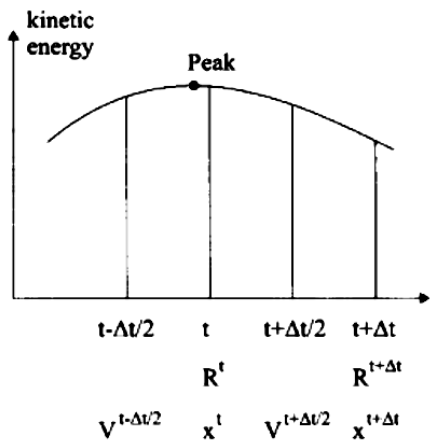


Fig. 2 Trace for a typical kinetic energy peak (Topping and Ivanyi 2008)

$$\dot{\mathbf{X}}^{n+1/2} = \frac{\tau}{2\mathbf{M}} \mathbf{R}^n \quad (14)$$

where the residual forces \mathbf{R}^n are calculated from the $\mathbf{X}^{n+1/2}$ displacement position. The trace for a typical kinetic energy peak is shown in Fig. 2.

2.4 Kinetic Dynamic Relaxation with fictitious Time step method (KDRT)

A new time step is developed in this section by performing error analysis on the kinetic DRM method (Rezaiee-Pajand and Rezaee 2014). This fictitious time step in each step is shown below

$$\Delta t^{n+1} = \frac{\left(\frac{2}{\Delta t^n} + \Delta t^n \lambda_1\right) - \sqrt{\left(\frac{2}{\Delta t^n} + \Delta t^n \lambda_1\right)^2 - 4\left(\frac{1}{\Delta t^n} - \Delta t^n \lambda_1\right)^2}}{2\left(\frac{1}{\Delta t^n} - \Delta t^n \lambda_1\right)^2} \quad (15)$$

where λ_1 shows the lowest eigenvalue of the matrix $\mathbf{M}^{-1}\mathbf{S}$. According to the Rayleigh's principle, the lowest natural frequency of the dynamic system is estimated from the following formula

$$\lambda_1 = \frac{(\mathbf{X}^n)^T \mathbf{S} \mathbf{X}^n}{(\mathbf{X}^n)^T \mathbf{M} \mathbf{X}^n} \quad (16)$$

3. Geometric stiffness matrix of three-dimensional membranes

A plane stress problem defines a two-dimensional (x, y) displacement field while a three-dimensional membrane in general defines a three-dimensional (x, y, z) displacement field. For the linear elastic problems, a membrane has no out-of-plane stiffness. That is not true in the nonlinear case. Just as the string (truss bar) has a "geometric" stiffness component normal to its axis, the nonlinear membrane has an out-of-plane "geometric" stiffness. That effect will be described below using the relationship from mechanics which gives the change $d\mathbf{F}$ of a force vector \mathbf{F} when subjected to a small rigid body rotation vector ω as (Levy and Spillers 2003, Spillers *et al.* 1992)

$$d\mathbf{F} = \omega \mathbf{F} = -\mathbf{F} \omega \quad (17)$$

This approach is possible since within small strain theory an out-of-plane displacement produces no strain in a membrane. According to Eq. (17), it should be clear that small, in-plane (z component) rotations are included within the geometric stiffness matrix. It is the effect of out-of-plane rotations (x, y components) which must be added to the existing formulation to complete the three-dimensional model. Given the x, y, z displacement components of the nodes of a typical finite element in Fig. 3, where the notations of a, c and e are also indicated, the out-of-plane rotation components ω_x, ω_y are

$$\mathbf{K}_G^e = \begin{bmatrix} 0 & \mathbf{A} & -\mathbf{A} \\ -\mathbf{A} & 0 & \mathbf{A} \\ \mathbf{A} & -\mathbf{A} & 0 \end{bmatrix} \quad (18)$$

$$\mathbf{A} = \frac{t}{2} \begin{bmatrix} -\tau_{xy} & \sigma_x \\ -\sigma_y & \tau_{xy} \end{bmatrix}$$

$$\omega_{x'} = \frac{1}{a} \left[(\delta_m)_{z'} - (\delta_i)_{z'} \left(1 - \frac{c}{e}\right) - \left((\delta_j)_{z'} \frac{c}{e} \right) \right] \quad (19)$$

$$\omega_{y'} = \frac{1}{e} \left[(\delta_j)_{z'} - (\delta_i)_{z'} \right] \quad (20)$$

It only now remains to construct a matrix representation of the incremental forces as in Eq. (18), produced by these rotations acting upon the element nodal forces. But since the rotation components of Eqs. (19) and (20) are linear in the displacements, the matrix ω can be written as

$$\omega = \mathbf{A}^* \delta^e \quad (21)$$

$$\begin{Bmatrix} \omega_{x'} \\ \omega_{y'} \\ \omega_{z'} \end{Bmatrix} = \begin{bmatrix} 0 & 0 & -\frac{e-c}{ae} & 0 & 0 & -\frac{c}{ae} & 0 & 0 & \frac{1}{a} \\ 0 & 0 & -\frac{1}{e} & 0 & 0 & \frac{1}{e} & 0 & 0 & 0 \\ 0 & 0 & 0 & 0 & 0 & 0 & 0 & 0 & 0 \end{bmatrix} \begin{Bmatrix} (\delta_i)_{x'} \\ (\delta_i)_{y'} \\ (\delta_i)_{z'} \\ (\delta_j)_{x'} \\ (\delta_j)_{y'} \\ (\delta_j)_{z'} \\ (\delta_m)_{x'} \\ (\delta_m)_{y'} \\ (\delta_m)_{z'} \end{Bmatrix} \quad (22)$$

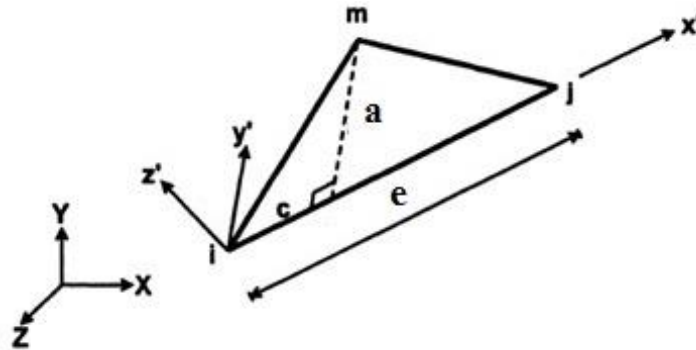


Fig. 3 Triangular finite element in its local coordinate system (Levy and Spillers 2003, Spillers *et al.* 1992)

The required contribution to the geometric stiffness matrix \mathbf{K}_G^* is then simplified as

$$\mathbf{K}_G^* = \begin{bmatrix} 0 & 0 & 0 & 0 & 0 & 0 & 0 & 0 & 0 \\ 0 & 0 & 0 & 0 & 0 & 0 & 0 & 0 & 0 \\ 0 & 0 & \alpha_i & 0 & 0 & \beta_i & 0 & 0 & \gamma_i \\ 0 & 0 & 0 & 0 & 0 & 0 & 0 & 0 & 0 \\ 0 & 0 & 0 & 0 & 0 & 0 & 0 & 0 & 0 \\ 0 & 0 & \alpha_j & 0 & 0 & \beta_j & 0 & 0 & \gamma_j \\ 0 & 0 & 0 & 0 & 0 & 0 & 0 & 0 & 0 \\ 0 & 0 & 0 & 0 & 0 & 0 & 0 & 0 & 0 \\ 0 & 0 & \alpha_m & 0 & 0 & \beta_m & 0 & 0 & \gamma_m \end{bmatrix} \quad (23)$$

where

$$\alpha_r = -\frac{e-c}{ae}(\mathbf{F}_r)_{y'} - \frac{1}{e}(\mathbf{F}_r)_{x'} ; r = i, j, m \quad (24)$$

$$\beta_r = -\frac{c}{ae}(\mathbf{F}_r)_{y'} + \frac{1}{e}(\mathbf{F}_r)_{x'} ; r = i, j, m \quad (25)$$

$$\gamma_r = \frac{1}{a}(\mathbf{F}_r)_{y'} ; r = i, j, m \quad (26)$$

4. Numerical examples

To study the efficiency of DRM methods, five different schemes summarized in the preceding Section 2 (DR, MDR1, MDR2, KDR, and KDRT) are considered. Geometrically nonlinear analysis is programmed to analyze these schemes. The initial value of the time step τ in the DRM procedures is set equal to 1. The acceptable residual errors are the same for all solutions and are equal to 10^{-4} . Also, the total number of iterations and the analysis durations are recorded for each case. These schemes had the same accuracy. However, they require the different number of iteration to achieve the desired accuracy. In order to compare these solvers, $G(i)$ as a performance index is calculated, as below (Rezaiee-Pajand *et al.* 2012)

$$G(i) = 0.6T(i) + 0.4It(i) \quad (27)$$

where $T(i)$ is the time index and $It(i)$ is the iteration index, which are considered as one of the methods that have minimum number of CPU time or iterations. These indexes are between zero and one, proportional to minimum values of iterations and time. In this paper, the weight of 0.6 for time analysis and 0.4 for the number of iteration are considered. As a result, the index of $G(i)$ is obtained for each DRM method, and the method having the maximum value of $G(i)$ is concluded as the most efficient method (see the paper by Rezaiee-Pajand *et al.* (2012) for more details). For

comparison, the models for the spherical cap and flat stretched membrane are introduced, as was done in the reference of Levy and Spillers (2003) where the models were analyzed using other numerical methods (not DRM). In this study, the same spherical cap and flat stretched membrane are analyzed using the five DRM methods summarized in Section 2.

4.1 Spherical cap

This example analyses a spherical cap for membrane. Fig. 4 shows a plan view of the analysis model. According to the Fig. 4 this model has 25 nodes that are subject to two different loadings. The cap has a radius of 4.76 in. (120.9 mm), a central angle of 10.9 degrees and a thickness of 0.01576 in. (0.4 mm). The Young's modulus and Poisson's ratio are 10,000 ksi (6,896.6 MPa) and 0.3, respectively. For the first loading, the load of 10,000 lb (44.48 kN) is applied at node 1, perpendicular to the plane of the membrane and in the positive direction, and for the second loading, the load of 10,000 lb (44.48 kN) is applied at all internal nodes. The pre-tension force in x and y directions are 250,000 psi (1724.14 MPa). The results of the calculations (the number of iterations and the CPU time) are listed, and the load-displacement curves for the spherical cap for the first and second loadings are shown in the foregoing subsections.

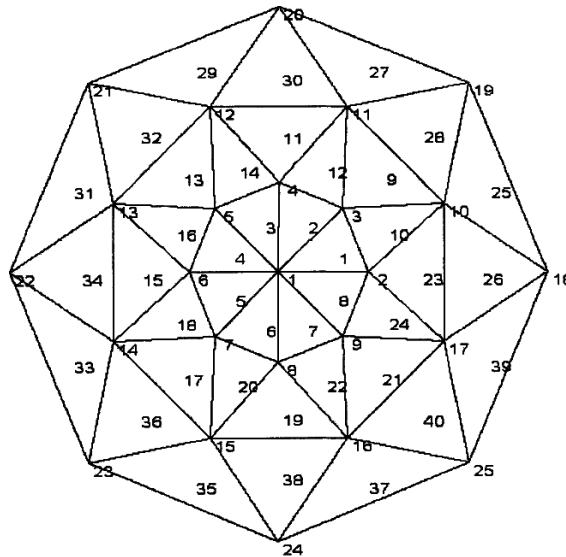


Fig. 4 Spherical membrane shell (Levy and Spillers 2003)

Table 1 Results of analysis for form-finding of spherical cap under first loading

Method of analysis	CPU time (sec)	$T(i)$	Number of iterations	$It(i)$	$G(i)$
DR	0.79	0.83	594	0.90	0.86
MDR1	0.71	0.93	569	0.94	0.94
MDR2	0.66	1	537	1	1
KDR	1.87	0.37	1347	0.40	0.38
KDRT	1.96	0.34	1436	0.37	0.35

4.1.1 Spherical cap under first loading

For this example, the form-finding of spherical membrane and load-displacement curve are shown in Figs. 5 and 6. The number of iterations in form-finding of this membrane for viscous damping methods are less than half of the iterations for the kinetic damping methods. So the viscous damping methods appear more stable and faster.

4.1.2 Spherical cap under second loading

According to Table 2, the $G(i)$ index is greater for viscous damping methods. This demonstrates better performance for the method. The form-finding under the second loading for a spherical membrane, and the load-displacement curve of this membrane are shown in Figs. 7 and 8, respectively.

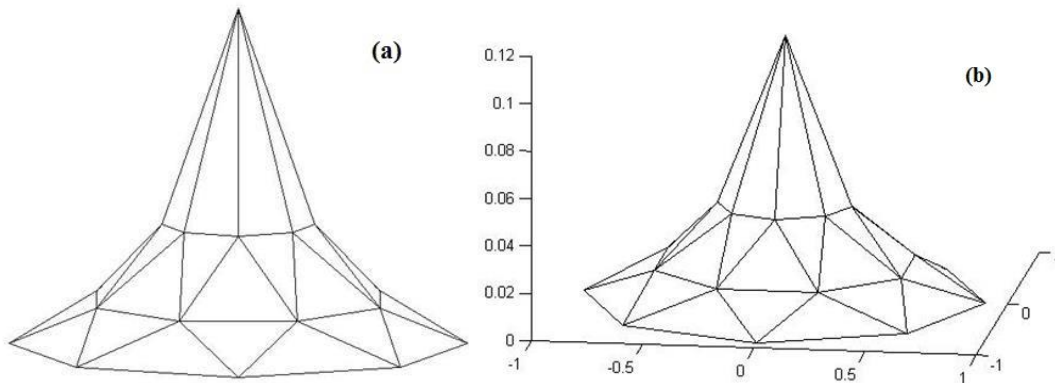


Fig. 5 (a) Two-dimensional view. (b) Perspective view of form-finding of spherical cap under first loading

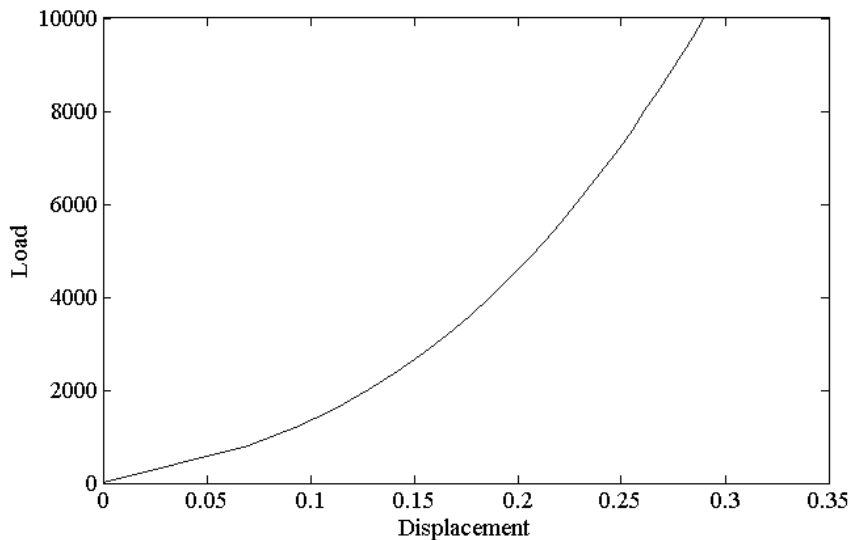


Fig. 6 Load-displacement curve for spherical cap under first loading (Load in lb and Displacement in in.; Conversion: 1 lb=4.448 N and 1 in.=25.4 mm)

Table 2 Results of analysis for form-finding of spherical cap under second loading

Method of analysis	CPU time (sec)	$T(i)$	Number of iterations	$It(i)$	$G(i)$
DR	0.51	0.84	401	0.83	0.84
MDR1	0.51	0.84	386	0.87	0.85
MDR2	0.43	1	334	1	1
KDR	2.27	0.19	1686	0.20	0.19
KDRT	2.07	0.21	1389	0.24	0.22

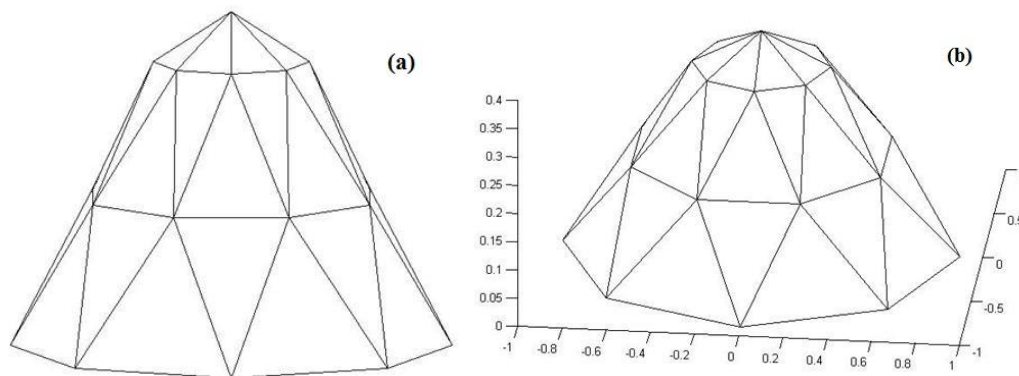


Fig. 7 (a) Two-dimensional view. (b) Perspective view of form-finding of spherical cap under second loading

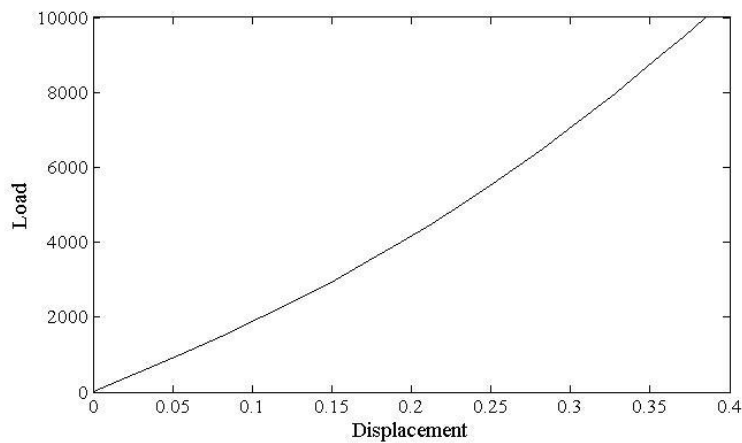


Fig. 8 Load-displacement curve for spherical cap under second loading (Load in lb and Displacement in in.; Conversion: 1 lb=4.448 N and 1 in.=25.4 mm)

4.2 Flat stretched membrane

Fig. 9 shows a plan view of the analysis model. This model has 81 nodes that are subject to three different loadings. The material properties of this example are the same as those of the

spherical cap example. As was for the first loading, a concentrated load of 10,000 lb (44.482 kN) is applied at the center of the membrane. The pre-tension force in x and y directions is 80,000 psi (551.72 MPa). For the second loading, only two midpoints of the plan are subject to concentrated loadings, and the pre-tension force in x and y directions is 800 psi (5.517 MPa). For this membrane, the load of 100 lb (0.4448 kN) is applied. Finally for the third loading, the force is applied at all internal nodes; the shapes of all four support sides are parabolic; and the pre-tension force is 80,000 psi (551.72 MPa). Results of analysis for these examples are given below.

Table 3 Results of analysis for form-finding of flat stretched membrane under first loading

Method of analysis	CPU time (sec)	$T(i)$	Number of iterations	$It(i)$	$G(i)$
DR	8.11	0.96	1312	0.95	0.95
MDR1	7.91	0.98	1254	0.99	0.99
MDR2	7.77	1	1240	1	1
KDR	9.92	0.78	2019	0.61	0.72
KDRT	10.51	0.74	2018	0.61	0.69

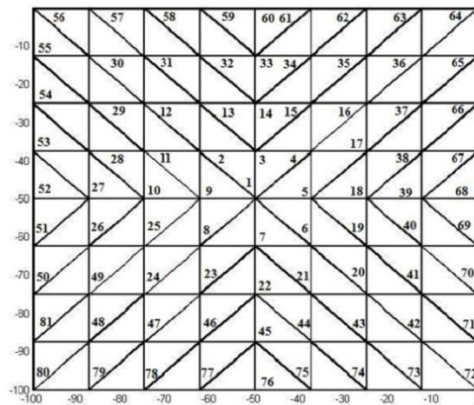


Fig. 9 Flat stretched membrane (Levy and Spillers 2003)

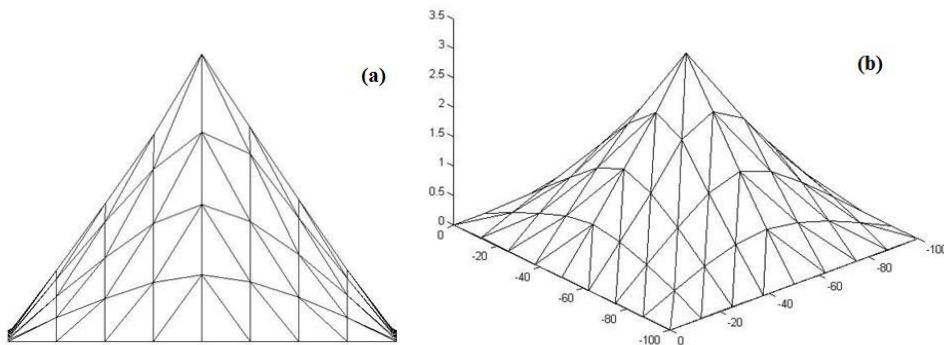


Fig. 10 (a) Two-dimensional view. (b) Perspective view of form-finding of flat stretched membrane under first loading

4.2.1 Flat stretched membrane under first loading

For finding shapes of the flat stretched membrane under the first loading MDR2 has the best performance in comparison to others. The form-finding of the flat stretched membrane in positive and negative loadings are shown in Fig. 10.

4.2.2 Flat stretched membrane under second loading

In this case, the performance of viscous damping is similar to the previous examples. However, the CPU times that required for nonlinear analysis of this example, in most methods, are equal to 10 seconds. Figs. 12 and 13 show the form-finding of membrane and load-displacement curve, respectively.

Table 4 Results of analysis for form-finding of flat stretched membrane under second loading

Method of analysis	CPU time (sec)	$T(i)$	Number of iterations	$It(i)$	$G(i)$
DR	10.70	0.93	1723	0.95	0.94
MDR1	10.14	0.99	1637	1	0.99
MDR2	10.00	1	1632	1	1
KDR	10.89	0.92	2369	0.69	0.83
KDRT	13.73	0.73	2709	0.6	0.68

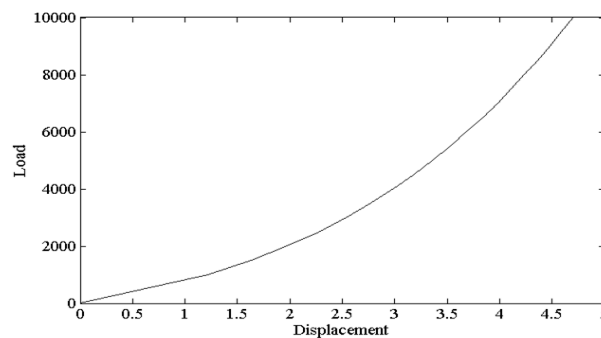


Fig. 11 Load-displacement curve for flat stretched membrane under first loading (Load in lb and Displacement in in.; Conversion: 1 lb=4.448 N and 1 in.=25.4 mm)

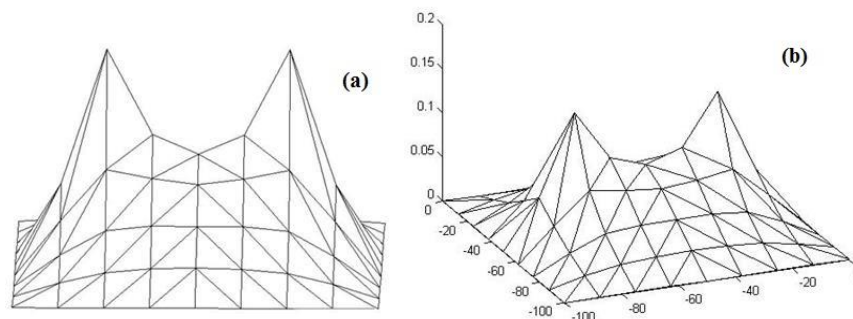


Fig. 12 (a) Two-dimensional view. (b) Perspective view of form-finding of flat stretched membrane under second loading

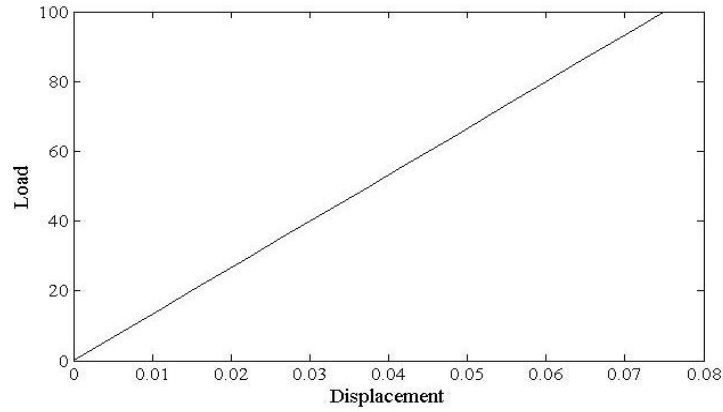


Fig. 13 (a) Load-displacement curve for flat stretched membrane under second loading (Load in lb and Displacement in in.; Conversion: 1 lb=4.448 N and 1 in.=25.4 mm)

4.2.3 Flat stretched membrane under third loading

Both the viscous and kinetic damping methods show good performance in form-finding of this loading of the flat stretched membrane. Fig. 14 shows form-finding of this example. The nonlinear behaviour for this membrane is depicted in Fig. 15.

Table 5 Results of analysis for form-finding of flat stretched membrane under third loading

Method of analysis	CPU time (sec)	$T(i)$	Number of iterations	$It(i)$	$G(i)$
DR	8.77	0.95	1209	0.95	0.95
MDR1	8.44	0.99	1156	0.99	0.99
MDR2	8.34	1	1143	1	1
KDR	12.54	0.67	2107	0.54	0.62
KDRT	8.54	0.98	1200	0.95	0.97

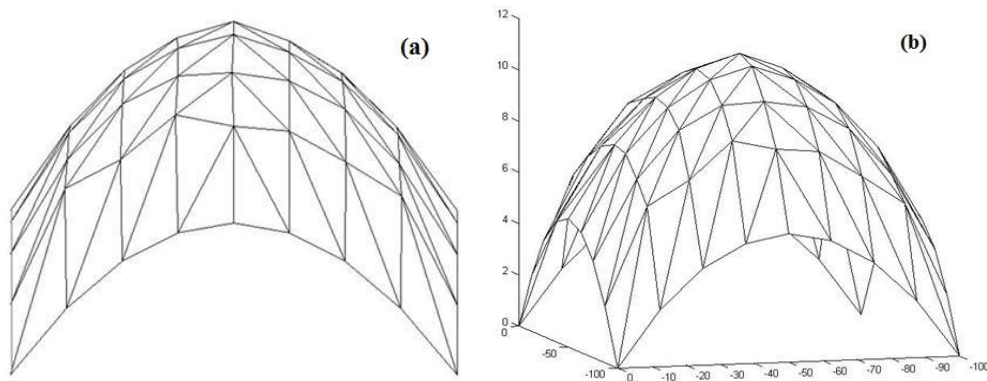


Fig. 14 (a) Two-dimensional view. (b) Perspective view of form-finding of flat stretched membrane under third loading

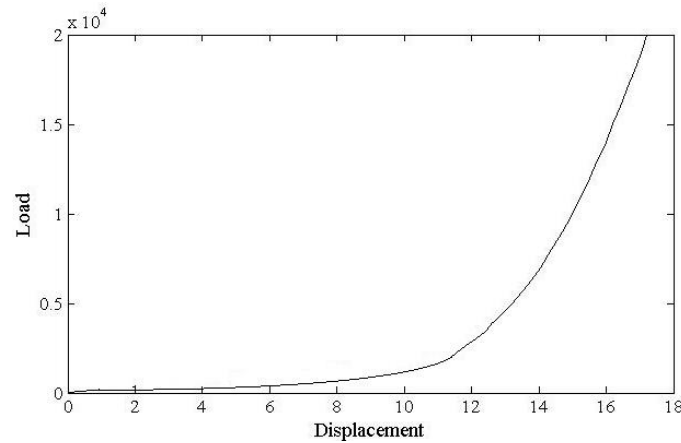


Fig. 15 Load-displacement curve for flat stretched membrane under third loading (Load in lb and Displacement in in.; Conversion: 1 lb=4.448 N and 1 in.=25.4 mm)

5. Conclusions

Solving the system of equations can be divided into two groups. The first uses matrix operations to solve equations, while the second group is the iterative process by which the initial response is improved. One of these iteration methods is the dynamic relaxation. In this article, different methods of the dynamic relaxation for nonlinear analysis which are required in finding shapes of membrane structures are studied. The run time of analysis of dynamic relaxation methods is in the range of a few seconds. According to the results of the analysis, dynamic relaxation methods with viscous damping are better than those with kinetic damping, as demonstrated by the performance index. The viscous damping methods require less time and number of iterations. In other words, the viscous damping methods have better performance than kinetic damping in finding shapes of membrane structures. Additionally, among the viscous damping methods investigated, the rate of convergence is increased the most by considering the damping and mass in the algorithms proposed by Rezaiee-Pajand and Alamatian (2010), which is the Modified Dynamic Relaxation method. Therefore, this method is suggested in this study as the best method among five DRMs that are available for form-finding of membrane structures.

References

- Alamatian, J. (2012), "A new formulation for fictitious mass of the dynamic relaxation method with kinetic damping", *Comput. Struct.*, **90-91**, 42-54.
- Al-Shawi, F.A.N. and Mardirosian, A.H. (1987), "An improved dynamic relaxation method for the analysis of plate bending problems", *Comput. Struct.*, **27**(2), 237-240.
- Barnes, M.R. (1988), "Form-finding and analysis of prestressed nets and membranes", *Comput. Struct.*, **30**(3), 685-695.
- Brew, J.S. and Brotton, D.M. (1971), "Non-linear structural analysis by dynamic relaxation", *Int. J. Numer. Methods Eng.*, **3**(4), 463-483.
- Bunce, J.W. (1972), "A note on the estimation of critical damping in dynamic relaxation", *Int. J. Numer. Methods Eng.*, **4**(2), 301-303.

- Cassell, A.C. and Hobbs, R.E. (1976), "Numerical stability of dynamic relaxation analysis of non-linear structures", *Int. J. Numer. Methods Eng.*, **10**(6), 1407-1410.
- Cundall, P.A. (1976), "Explicit finite-difference method in geomechanics", *Proceedings of the International Conference on Numerical Methods in Geomechanics*, Blacksburg, 132-150.
- Frankel, S.P. (1950), "Convergence rates of iterative treatments of partial differential equations", *Math. Tables Aids Comput.*, **4**(30), 65-75.
- Frieze, P.A., Hobbs, R.E. and Dowling, P.J. (1978), "Application of dynamic relaxation to the large deflection elasto-plastic analysis of plates", *Comput. Struct.*, **8**(2), 301-310.
- Kadkhodayan, M., Alamatian, J. and Turvey, G.J. (2008), "A new fictitious time for the dynamic relaxation (DXDR) method", *Int. J. Numer. Methods Eng.*, **74**(6), 996-1018.
- Levy, R. and Spillers, W.R. (2003), *Analysis of Geometrically Nonlinear Structures*, 2nd edition. ed. Springer, Dordrecht, New York.
- Lewis, W.J. (2003), *Tension Structures: Form and Behaviour*, Thomas Telford.
- Munjiza, A., Owen, D.R.J. and Crook, A.J.L. (1998), "An M(M-1K)m proportional damping in explicit integration of dynamic structural systems", *Int. J. Numer. Methods Eng.*, **41**(7), 1277-1296.
- Nabaei, S.S., Baverel, O. and Weinand, Y. (2013), "Mechanical form-finding of the timber fabric structures with dynamic relaxation method", *Int. J. Space Struct.*, **28**(3-4), 197-214.
- Otter, J.R.H. (1966), "Dynamic relaxation compared with other iterative finite difference methods", *Nucl. Eng. Des.*, **3**(1), 183-185.
- Papadrakakis, M. (1981), "A method for the automatic evaluation of the dynamic relaxation parameters", *Comput. Methods Appl. Mech. Eng.*, **25**(1), 35-48.
- Qiang, S. (1988), "An adaptive dynamic relaxation method for nonlinear problems", *Comput. Struct., Special Issue: Comput. Eng. Mech.*, **30**(4), 855-859.
- Rezaiee-Pajand, M. and Alamatian, J. (2010), "The dynamic relaxation method using new formulation for fictitious mass and damping", *Struct. Eng. Mech.*, **34**(1), 109-133.
- Rezaiee-Pajand, M. and Alamatian, J. (2005), "Best time step for geometric nonlinear analysis using dynamic relaxation", *Modares J. Civ. Eng.*, 19.
- Rezaiee-Pajand, M. and Taghavian-Hakkak, M. (2006), "Nonlinear analysis of truss structures using dynamic relaxation (research note)", *Int. J. Eng. - Trans. B Appl.*, **19**(1), 11-12.
- Rezaiee-pajand, M., Kadkhodayan, M., Alamatian, J. and Zhang, L.C. (2011), "A new method of fictitious viscous damping determination for the dynamic relaxation method", *Comput. Struct.*, **89**(9-10), 783-794.
- Rezaiee-Pajand, M. and Rezaee, H. (2014), "Fictitious time step for the kinetic dynamic relaxation method", *Mech. Adv. Mater. Struct.*, **21**(8), 631-644.
- Rezaiee-Pajand, M. and Sarafrazi, S.R. (2011), "Nonlinear dynamic structural analysis using dynamic relaxation with zero damping", *Comput. Struct.*, **89**(13-14), 1274-1285.
- Rezaiee-Pajand, M. and Sarafrazi, S.R. (2010), "Nonlinear structural analysis using dynamic relaxation method with improved convergence rate", *Int. J. Comput. Method.*, **7**(4), 627-654.
- Rezaiee-Pajand, M., Sarafrazi, S.R. and Rezaiee, H. (2012), "Efficiency of dynamic relaxation methods in nonlinear analysis of truss and frame structures", *Comput. Struct.*, **112-113**, 295-310.
- Rushton, K.R. (1969), "Dynamic-relaxation solution for the large deflection of plates with specified boundary stresses", *J. Strain Anal. Eng. Des.*, **4**(2), 75-80.
- Spillers, W.R., Schlogel, M. and Pilla, D. (1992), "A simple membrane finite element", *Comput. Struct.*, **45**(1), 181-183.
- Topping, B.H.V. and Ivanyi, P. (2008), *Computer aided design of cable membrane structures*, Saxe-Coburg Publications, Kippen, Stirlingshire, Scotland.
- Veenendaal, D. and Block, P. (2012), "An overview and comparison of structural form finding methods for general networks", *Int. J. Solid. Struct.*, **49**(26), 3741-3753.
- Wood, R.D. (2002), "A simple technique for controlling element distortion in dynamic relaxation form-finding of tension membranes", *Comput. Struct.*, **80**(27-30), 2115-2120.
- Wood, W.L. (1971), "Note on dynamic relaxation", *Int. J. Numer. Methods Eng.*, **3**(1), 145-147.
- Xu, R., Li, D.X., Liu, W., Jiang, J.P., Liao, Y.H. and Wang, J. (2015), "Modified nonlinear force density

method for form-finding of membrane SAR antenna”, *Struct. Eng. Mech.*, **54**(6), 1045-1059.
Zhang, L.G. and Yu, T.X. (1989), “Modified adaptive dynamic relaxation method and its application to elastic-plastic bending and wrinkling of circular plates”, *Comput. Struct.*, **33**(2), 609-614.

CC